Journal of Innovative Technology, Vol. 8, No. 2, pp. 69-85, September 2026
http://doi.org/10.29424/JIT.202609_8(2).0007

Numerical computing schemes for Arneodo's chaotic system: A comparative study between Adams, BDF, implicit and explicit Runge-Kutta methods

Muhammad Haseeb [1], Muhammad Asif Zahoor Raja [2*]

ABSTRACT

Now a days analyzing the various numerical computing methods play an essential role to enhance efficiency, accuracy, stability, robustness, and convergence for solving variety of computational problems arising in different scientific and engineering domains. Analyzing various numerical computing methods helpful to understand their capacity and ability to solve a mathematical problem and accordingly ranks the suitable in practice. The viable numerical computing helps in the process of inspecting data for better insights, design formulation, complicated structure modelling, and sustainable well-grounded standards for choosing an application with appropriate algorithm for numerical integration. Renowned numerical computing paradigm are exploited for solving the systems governed with differential equations to enhance the core components of mathematical sciences such as structural design analysis with bioinformatics, genetics, microelectromechanical systems (MEMS), chaotic electronic circuits, construction management, aerospace based satellite systems, fluid simulations, cryptocurrency trend analysis, weather forecasting, global warming simulations, risk management, stock market prediction and chaos problems etc.. The aim of presented study is to investigate the deterministic numerical computing paradigm to analysis the mathematical model of Arneodo's system representing the chaotic complex oscillations and the bifurcation behavior of dynamical systems. In the presented study, four prestigious numerical computing methods, i.e., Adams numerical computing (ANC) procedure, finite difference on backward differential formulas (FD-BDF) method, explicit Runge-Kutta (E-RK), and implicit Runge-Kutta (I-RK), are exploited for complex chaotic structure interaction for Arneodo's system across transverse deviation dynamics. Numerical outcomes of these deterministic solvers are used to predict the behavior of bifurcation and the oscillations of all possible trajectories of the Arneodo's system. The residual results confirm that all numerical methods successfully capture the bounded chaotic behavior of the Arneodo's system effectively.

Keywords: Arneodo's System; Numerical computing; Adams method; Runge-Kutta methods; Chaotic Dynamics.

1. INTRODUCTION

Numerical computing involves large number of exhausting arithmetic calculations, i.e., the process of arithmetic operations, especially for addition, subtraction, multiplication, division and functional evaluations. The approximation of complex mathematical calculations is required for fast and efficient computing devices. The process of numerical computing consists of selecting suitable numerical methods formulated into specific models, aiding in proficient solution finding and validation. Thus, plays a crucial role in computing real life engineering problems and follows the computing phenomenon utilizing discrete and continuous information. The information highlighted in Table 1 represents the significance of numerical computing publications in various scientific fields globally that are listed as applied mathematics, mechanics, engineering electrical electronic and computer science interdisciplinary applications for the query on web of science (WoS) with topic "numerical computing". While USA, China, France and Germany are leading countries with the publication of 28188, 23866, 10636 and 9023, respectively in the domain of numerical computing as per statistics visually showcased in Figure 1. Figure 2 depicts the increasing annual trend of publications in domain of numerical computing per annum. The interest of vast communities in this domain highlights immense significance of numerical computing in modern era.

Table 1 Summary of Publication Selection across Web of Science categories

Web of Science Categories	Record Count	% of 113,749
Applied Mathematics	15933	14.007
Mechanics	14355	12.62
Engineering Electrical Electronic	11457	10.072
Computer Science Interdisciplinary Applications	8604	7.564
Mathematics Interdisciplinary Applications	7504	6.597
Engineering Mechanical	7320	6.435
Engineering Multidisciplinary	6552	5.76
Physics Mathematical	6516	5.728
Astronomy Astrophysics	5592	4.916

Manuscript received June 12, 2026; revised June 29, 2026; accepted July 23, 2026.

[1] PhD Scholar, Graduate School of Engineering Science and Technology, National Yunlin University of Science and Technology, Taiwan R.O.C.

[2*] Professor (corresponding author), Graduate School of Engineering Science and Technology, National Yunlin University of Science and Technology, Taiwan R.O.C. (email: rajamaz@yuntech.edu.tw)

Web of Science Categories	Record Count	% of 113,749
Materials Science Multidisciplinary	5568	4.895
Physics Fluids Plasmas	4736	4.164
Physics Applied	4724	4.153
Telecommunications	4719	4.149
Engineering Civil	4439	3.902
Physics Multidisciplinary	3941	3.465
Mathematics	3811	3.35
Thermodynamics	3737	3.285
Geosciences Multidisciplinary	3195	2.809

Web of Science Categories	Record Count	% of 113,749
Optics	3140	2.76
Computer Science Information Systems	3130	2.752
Operations Research Management Science	2980	2.62
Computer Science Theory Methods	2861	2.515
Geochemistry Geophysics	2844	2.5
Automation Control Systems	2777	2.441
Physics Particles Fields	2709	2.382

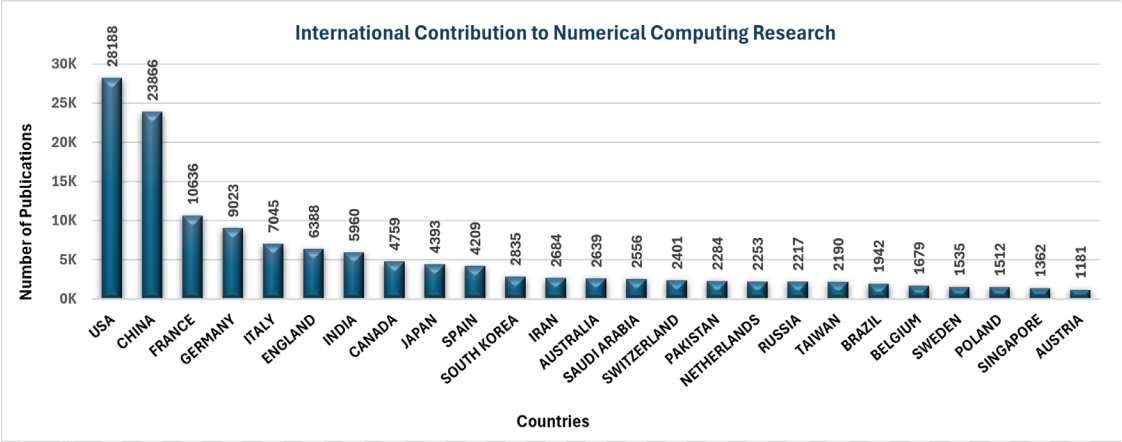


Fig. 1 WoS Statistics for Leading Country Contributing to Numerical Computing Research

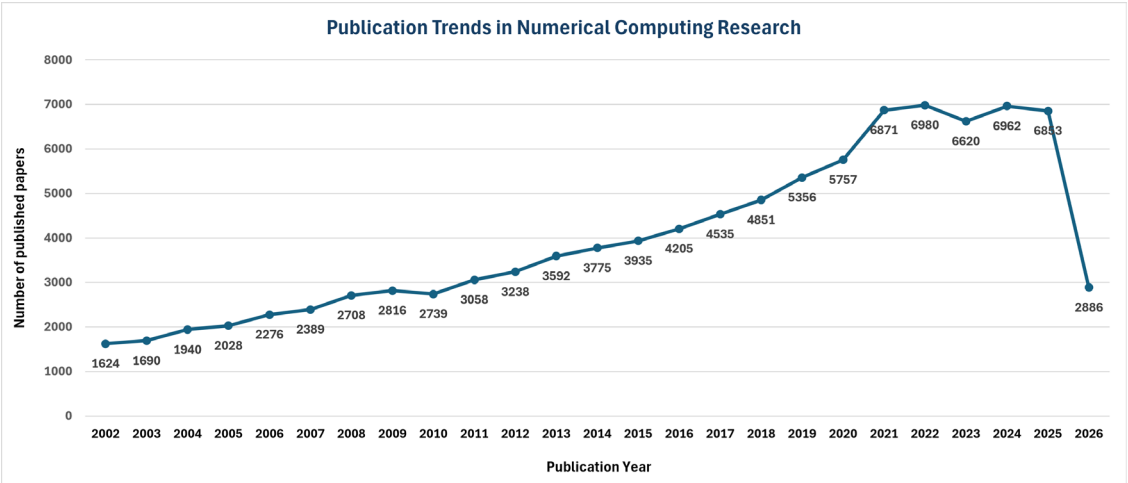


Fig. 2 WoS Statistics for Number of Publications Per Annum in Numerical Computing Research

Chaotic systems have strong nonlinearities and stiffness and therefore require state-of-the-art numerical computing algorithms to solve them. Henceforth, continuous efforts of the research community are exerted to explore, visualize, quantify, and develop new variants of existing computing schemes. The root of chaotic behavior is generally represented by differential equations [1] because chaotic systems are deterministic nonlinear starting state with one possible outcome that displays aperiodic behavior over time and extremely sensitive to small changes in the initial conditions [2]. Chaos is not random but complicated representation of the system due to which the researchers tried to find order in the chaos using shapes of strange attractors [3] that show the hidden patterns. The study of how tiny changes lead to huge unpredictable, yet patterned outcomes is introduced by pioneer of chaos theory

that is Henri Poincare done in the late 19th century [4]. Poincare's meticulous calculations unveil the dynamics of economic field by implementing the predictability of complex chaotic system utilizing in meteorology field [5]. In 1981, Arneodo's system was introduced by Alain Arneodo that preserves symmetry by studying three-dimensional differential systems and is one of prestigious nonlinear chaotic systems describing complex oscillations and the bifurcation behavior for dynamical systems [6]. Chaotic systems play an important role in natural sciences such as forecasting complex weather patterns [7], analyzing turbulent flow in fluid dynamics [8], cryptography [9] and information security [10]. The studies recently reported including chaotic dynamics have been useful in autonomous behavior of robots [11] to interact with humans [12], analogue digital electronic circuits [13], field programmable gate arrays [14], macroeconomic agents [15], real-life microprocessors modelling systems [16], secure communications [17], antenna arrays [18], radar systems[19], biomedical engineering [20], civil infrastructure [21], mechanical[22], robot kinematics [23], power systems [24], chaotic optimization techniques [25], rescue operations [26], mine sweeping [27], lawn mowing tasks [28] and electro-hydraulic control systems [29].

The chaotic Arneodo's system is crucial in study of nonlinear mechanical oscillators for analyzing vibrating beam and micro-electromechanical systems [30], chaotic electronic circuits problems [31], image encryption applications [32], secure communication in microcontrollers [33], projective synchronization control [34], secure encryption of biomedical images [35], data security [36], order modulation for chaos control [37] and vice versa. Arneodo's system plays pivotal role in various physical and engineering systems due to its cubic nonlinear term which represents nonlinear restoring force. Figure 3 represents the leading countries China, USA, France and England with the publications record of 204,180,75 and 61 that is retrieved from Web of Science (WoS) using query "numerical computing" (topic) and "chaotic system" (all fields) with total outcome retrieved 925 publications. Similarly, Figure 4 represents the global publications record from WoS with query "numerical computing" (topic) and "Arneodo system" (all fields) retrieved 17 records of France, Iran and China having publications on Arneodo system. Figure 5 exhibiting same query but representing the WoS Categories result. Interest shown by researchers worldwide highlights the importance of Arneodo's system in the various domains as well as lead us to exploit numerical computing paradigms for in depth understanding of the complex dynamics with the help of comparative studies.

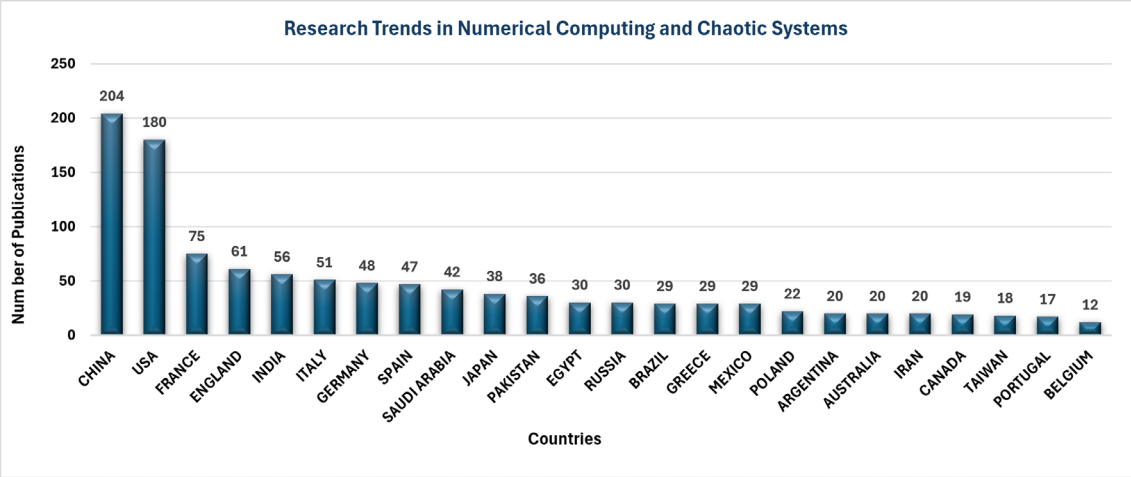


Fig. 3 WoS Statistical Analysis of Publications on Numerical Computing and Chaotic Systems (N = 925)

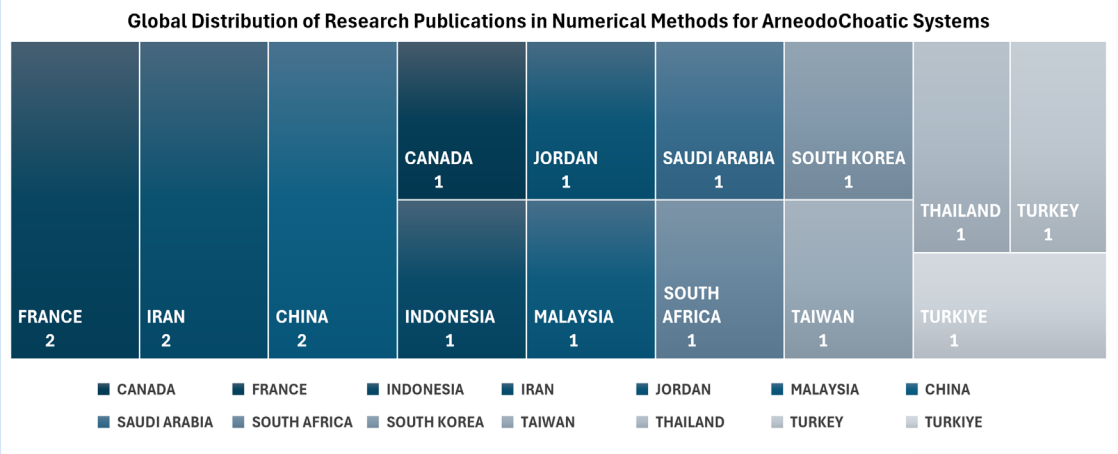


Fig. 4 WoS core collection of Global Distribution on Publications of Numerical Computing and Chaotic Systems

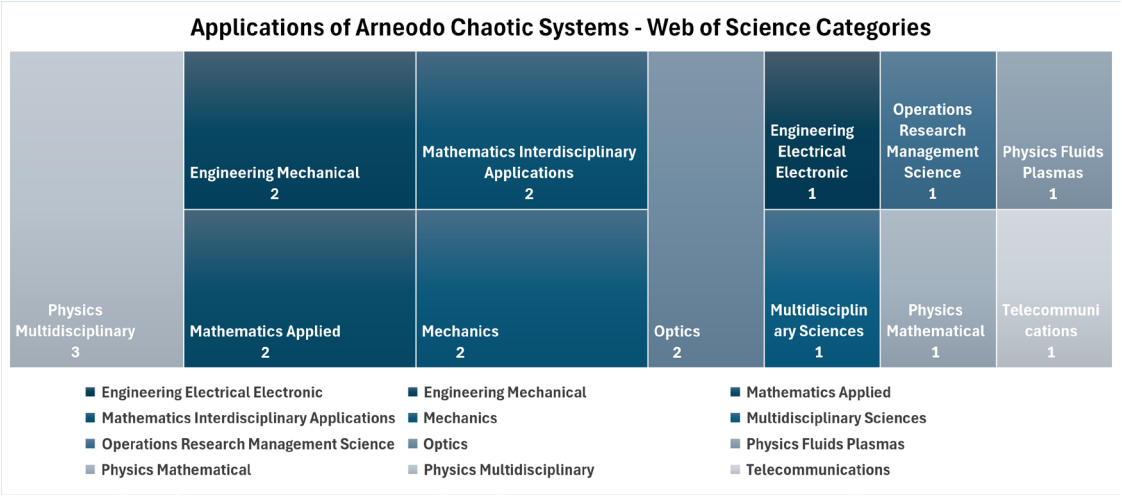


Fig. 5 WoS core collection of global distribution applications of numerical computing and chaotic systems

The salient features of this study are:

- The complex nonlinear Arneodo's chaotic attractor is numerically simulated using Adams, BDF, E-RK and I-RK numerical attractor.
- The time evolution trajectories of Arneodo's systems are visualized along with error analysis considering Adams the reference numerical solution.
- The chaotic attractors of the three compartmental Arneodo's system are effectively simulated by all four numerical methods.
- Error analysis reveals that Arneodo's chaotic attractor is formulated by all four numerical methods, while the error stays low throughout.

The remaining research article is structures as follows: Section 2 provides mathematical formulation of Arneodo's system capturing the chaotic behavior. Section 3 provides guidance on the numerical methods that are Adams' and Backward Differentiation Formula (BDF) methods, E-RK, and I-RK implemented in computing the nonlinear differential Arneodo's system. Section 4 demonstrates the results and discussion by showcasing outcomes in tabular and graphical form. Lastly, Section 5 presents the conclusion of this study and discusses possible future scope.

2. MATHEMATICAL MODEL

In this section, the model presented by Arneodo et al in 1981 through his studies on "Possible New Strange Attractors with Spiral Structure" [4] governed with a three-dimensional nonlinear differential system [38] that exhibit chaotic behavior, oscillations and bifurcation [39]. Arneodo system is considered benchmark nonlinear chaotic model in engineering, mathematics, physics, and computational research. The Arneodo system is expressed as:

$$\begin{cases} \dot{X} = Y \\ \dot{Y} = Z \\ \dot{Z} = -\alpha X - \beta Y - \gamma Z + \delta X^3 \end{cases} \quad (1)$$

X, Y, and Z are state variable and α, β, γ, and δ are controlling parameters as defined in Table 2 [4]. Where δX^3 acts like restoring force term and the initial conditions are (X[0], Y[0], Z[0])=(-2,0.1,1), with parameters (α, β, γ, δ)=(-5.5,3.5,1, -1) [4]. Table 2 provides a brief parametric description of the Arneodo's system while a state diagram representation of the Arneodo's system is provided in Figure 6.

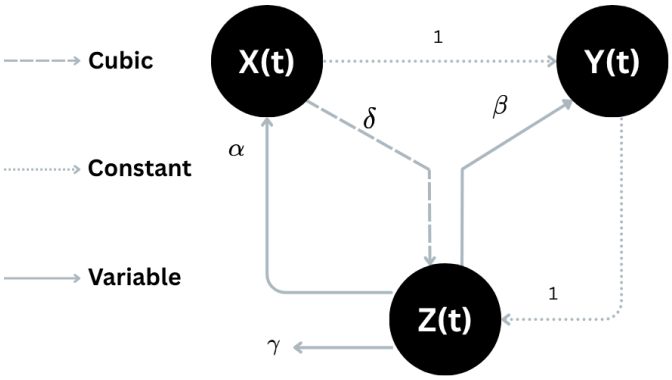


Fig. 6 State Diagram of Arneodo's system

Table 2 Description of the components within the Arneodo's system.

Component	Description
X	Displacement
Y	Velocity
Z	Acceleration
α	Controlling stiffness
β	Stabilized motion
γ	Influence on chaotic intensity
δ	restoring force/nonlinear strength

3. NUMERICAL METHODS

This section describes numerical investigation of the chaotic behaviors of the Arneodo's system with dynamical behavior of the governed by the following i) nonlinear ordinary differential equations: we applied four prestigious numerical methods including

the Adams, BDF, E-RK and I-RK to solve the Arneodo's system numerically.

3.1 Adams Numerical Computing Procedure

Adams numerical computing procedure (ANC) uses past data points to simulate the next solution efficiently due to its multi-step technique. There are two main types of Adams methods, namely Adams-Bashforth (Explicit) method and Adams-Moulton (Implicit) methods. Adams methods are commonly utilized because its a highly efficient method. Adams-Bashforth (explicit) and Adams-Moulton (implicit predictor corrector) are more accurate with comparatively higher cost when compared with Runge-Kutta methods.

Assume a differential equation of the form:

$$\frac{dy}{dt} = f(t, y) \tag{2}$$

Integrate both sides over the 3nterval:

$$y(t_{n+1}) - y(t_n) = \int_{t_n}^{t_{n+1}} f(t, y(t))dt \tag{3}$$

$$y_{n+1} = y_n + \int_{t_n}^{t_{n+1}} f(t, y(t))dt \tag{4}$$

3.2 Adams-Bashforth Method

The Adams-Bashforth method predicts next value using previous slopes:

$$y_{n+1} = y_n + \frac{h}{2}(3f_n - f_{n-1}) \tag{5}$$

where: f_n and f_{n-1} are already know.

3.3 Adams-Moulton Method (Implicit)

In the implicit method, the unknown values are inside the formula including the future point itself:

$$y_{n+1} = y_n + \frac{h}{2}(f_n - f_{n-1}) \tag{6}$$

Then, we can clearly see

$$f_{n+1} = f(t_{n+1}, y_{n+1}) \tag{7}$$

where y_{n+1} is unknown.

3.4 BDF Method

BDF methods are utilized to solve stiff differential equations and are used in several applications of biological sciences and numerous other fields. It is a fundamentally different method when compared with Adams numerical computing procedure. BDF computes the solution of y(t) by means of differentiation as well as polynomial interpolation.

For derivation of the 2-Step BDF method. Let's suppose that y(t) is interpolated using the following points:

$$(t_{n+1}, y_{n+1}), (t_{n,}, y_n), (t_{n-1}, y_{n-1}) \tag{8}$$

Formulate the quadratic polynomial interpolation:

$$P(t) \tag{9}$$

Differentiate the polynomial and establish the new point at t_{n+1}:

$$P'(t_{n+1}) \approx y'(t_{n+1}) = f(t_{n+1}, y_{n+1}) \tag{10}$$

Since

$$y'(t_{n+1}) = f(t_{n+1}, y_{n+1}), \tag{11}$$

We obtain

$$\frac{3y_{n+1} - 4y_n + y_{n-1}}{2h} = f_{n+1} \tag{12}$$

multiple by 2h:

$$3y_{n+1} - 4y_n + y_{n-1} = 2hf_{n+1} \tag{13}$$

Here is the 2-step Backward Differentiation Formula:

$$y_{n+1} = \frac{4}{3}y_n - \frac{1}{3}y_{n-1} + \frac{2}{3}hf_{n+1} \tag{14}$$

The generic formula for BDF shown as:

$$\sum_{k=0}^{s} \alpha_k y_{n+k} = h\beta f(t_{n+s}, y_{n+s}) \tag{15}$$

then for k-step BDF formula can be written as

$$\sum_{j=0}^{k} \alpha_j y_{n+1-j} = hf(t_{n+1}, y_{n+1}) \tag{16}$$

In this paper, both numerical methods (Adams and BDF) are utilized to numerical solution for complex nonlinear Arneodo's system. Throughout this study, Adams method is considered the reference solution which is compared with BDF methodology.

3.5 E-RK Numerical Method

Explicit Runge-Kutta methods are usually used to solve ordinary differential equations. It's a famous technique for numerical solutions of many initial-value problems. It is one of the methods from the family of Runge–Kutta (RK) methods. An historical overview of this approach for solving differential equations is given by Butcher [40]. The E-RK method is used to solve an initial value problem of the form

$$\frac{dy}{dt} = f(t, y(t)), y(t_0) = y_0 \tag{17}$$

Now we pick a step-size h>0and formulate the method:

$$k_1 = f(t_n, y_n) \tag{18}$$

$$k_2 = f\left(t_n + \frac{h}{2}, y_n + \frac{hk_1}{2}\right) \tag{19}$$

$$k_3 = f\left(t_n + \frac{h}{2}, y_n + \frac{hk_2}{2}\right) \tag{20}$$

$$k_4 = f\left(t_n + h, y_n + hk_3\right) \tag{21}$$

E-RK method has played a pivotal role in the fields of engineering, fluid dynamics, robotics, aerospace, and chaos theory due to its accuracy and simplicity.

3.6 I-RK Numerical Method

The implicit form of Runge-Kutta is also utilized to solve both ordinary differential equations (ODE's) and differential algebraic equations (DAE's). This method is particularly efficient in numerically solving stiff differential equations where explicit method requires extremely small-time steps. Consider the initial value problem:

$$\frac{dy}{dt} = f(t, y(t)), y(t_0) = y_0 \tag{22}$$

Where numerical approximation y_{n+1} at

$$t_{n+1} = t_n + h \tag{23}$$

$$k_i = f\left(t_n + c_i h, y_n + h\sum_{j=1}^{s} aijkj\right), i = 1, ..., s. \tag{24}$$

$$y_{n+1} = y_n + h\sum_{i=1}^{s} b_i k_i \tag{25}$$

This is the generalized form of the famous I-RK method.

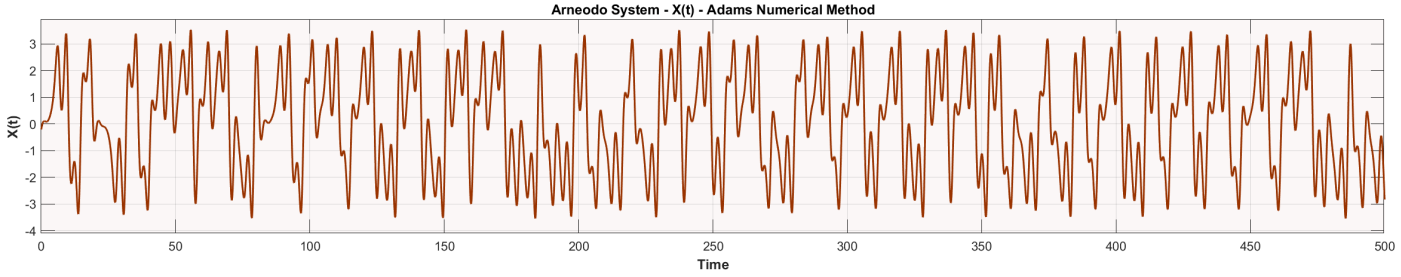
4. RESULTS AND DISCUSSION

This section provides discussion on the numerical study of complex nonlinear Arneodo's system. For Case-I Using parameters (α, β, γ, δ) = (-5.5,3.5,1, -1) described in Section 2 with Adams, BDF, E-RK and I-RK method. The behavior of X(t), Y(t), and Z(t) with $0 \le t \le 500$-time interval in Figures 7, 8 and 9 where Adams is the reference numerical solution. In Figure (2a), Arneodo's X(t) compartment over the simulated interval $0 \le t \le 500$ using Adams numerical approach is clearly confined within a finite amplitude range but exhibiting irregular and chaotic oscillations between the range of -4 to + 3.5. To further interrogate the temporal behavior, three different short intervals $0 \le t \le 150$, $0 \le t \le 100$, and $0 \le t \le 50$ are graphically provided in Figures (7b), (7c) and (7d) respectively. These time intervals highlight the steady state, while the longer intervals show the continuousness of aperiodic oscillations. These observations indicate that the numerical solution captures the characteristic bounded and irregular behavior of Arneodo's chaotic system while Figure (8a) exhibit trajectory evolution of Arneodo's Y(t) compartment over the simulated interval $0 \le t \le 500$ using Adams numerical approach is clearly confined within a finite amplitude range but exhibiting irregular and chaotic oscillations between the range of -6 to +6. To further interrogate the temporal behavior, three different short intervals $0 \le t \le 150$, $0 \le t \le 100$, and $0 \le t \le 50$ are graphically provided in Figures (3b), (3c) and (3d) respectively, similarly Figure (9a) Arneodo's Z(t) compartment over the simulated interval $0 \le t \le 500$ using Adams method exhibiting huge deviation, around -15 to +15. To further interrogate the temporal behavior, three different short intervals $0 \le t \le 150$, $0 \le t \le 100$, and $0 \le t \le 50$ are graphically provided in Figures (9b), (9c) and (9d) respectively. Its indicate oscillatory irregular behavior with persistence around the zero. No steady-state equilibrium with the topmost variations observed in Z(t). That sharp peaks in Z(t) represent the speedy change in the trajectory. Rest of the methods were implemented with same interval of time $0 \le t \le 500$. Figure 10 represents the response trajectories X(t), Y(t), and Z(t) using BDF numerical method. Figure (10a) representing that X(t) compartment over the simulated interval $0 \le t \le 500$ oscillate around -4 to +4, with three different short intervals $0 \le t \le 150$, $0 \le t \le 100$, and $0 \le t \le 50$ are graphically provided in Figures (10b), (10c) and (10d) respectively while Figure (11a), Arneodo's Y(t) compartment over the simulated interval $0 \le t \le 500$ using Adams numerical approach is clearly confined within a finite amplitude range but exhibiting irregular and chaotic oscillations between the range of -6 to +6. To further interrogate the temporal behavior, three different short intervals $0 \le t \le 150$, $0 \le t \le 100$, and $0 \le t \le 50$ are graphically provided in Figures (7b), (7c) and (7d).

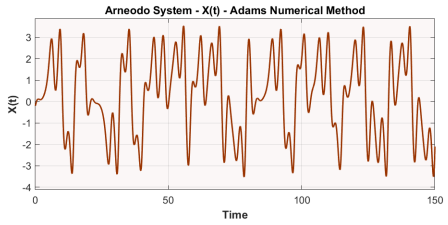
Similarly, Figure (12a) Arneodo's Z(t) compartment over the simulated interval $0 \le t \le 500$ using Adams method exhibiting huge deviation, around -15 to +15. To further interrogate the temporal behavior, three different short intervals $0 \le t \le 150$, $0 \le t \le 100$, and $0 \le t \le 50$ are graphically provided in Figures (12b), (12c), and (12d).In Figure (13a) obtain from E-RK method were X(t) demonstrate irregular oscillate response remains between -4 to +4 with three different short intervals $0 \le t \le 150$, $0 \le t \le 100$, and $0 \le t \le 50$ are graphically provided in Figures (13b), (13c) and (13d).and Figure 14 Y(t) varies between -8 to +6 with three different short intervals $0 \le t \le 150$, $0 \le t \le 100$, and $0 \le t \le 50$ are graphically provided in Figures (14b), (14c) and (14d) respectively. In Figure (15a), Arneodo's Z(t) compartment over the simulated interval $0 \le t \le 500$ using BDF numerical method exhibiting huge deviation, around -15 to +15. To further interrogate the temporal behavior, three different short intervals $0 \le t \le 150$, $0 \le t \le 100$, and $0 \le t \le 50$ are graphically provided in Figures (15b), (15c) and (15d). Its indicate oscillatory irregular behavior with persistence around zero with the topmost variations observed in Z(t). That sharp peaks in Z(t) represent the speedy change in the trajectory. Similarly Figure (16a) obtained by I-RK method were X(t) demonstrate irregular oscillate response remains between -4 to +4 with three different short intervals $0 \le t \le 150$, $0 \le t \le 100$, and $0 \le t \le 50$ are graphically provided in Figures (16b), (16c) and (16d).In Figure (17a) the trajectory evolution of function Y(t) of Arneodo's system using I-RK varies around -6 to +6 with three different short intervals $0 \le t \le 150$, $0 \le t \le 100$, and $0 \le t \le 50$ are graphically provided in Figures (17b), (17c) and (17d) respectively. In Figure (18a), Arneodo's Z(t) compartment using I-RK numerical method demonstrates the large amplitude range between -15 to +15 with huge deviation. To further interrogate the temporal behavior, three different short intervals $0 \le t \le 150$, $0 \le t \le 100$, and $0 \le t \le 50$ are graphically provided in Figures (18b), (18c) and (18d). It indicates oscillatory irregular behavior with persistence around zero. Comparison with all methods has demonstrated stronger spectrum chaotic oscillatory response than X(t), Y(t) it represents the nonlinear effect while X(t) remains within a smaller range, Z(t) oscillates approximately between ±15 under the selected parameter values. It indicates that the third state variable has a stronger dynamic response However, despite its larger amplitude, the response remains bounded and does not diverge, which confirms the chaotic nature of the system.

Exhaustive error analysis between reference Adams Numerical Computing (ANC) Procedure across various numerical techniques including BDF, E-RK and I-RK for the X(t), Y(t) and Z(t) components of Arneodo's chaotic system dynamics across the time domain $0 \le t \le 500$ is showcased in Figures 19, 20 and 21 correspondingly. Figure (19a) exhibits absolute error between Adams Numerical Computing (ANC) Procedure and the other numerical solutions such as BDF, E-RK, and I-RK schemes. In Fig-

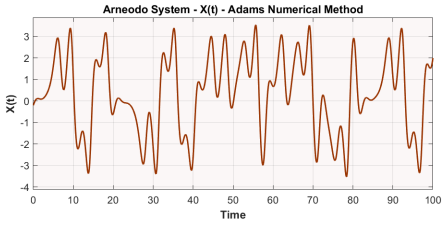
ure (19a), showing solver-dependent deviations caused by chaotic sensitivity with the minimum residuals of Adams vs BDF in Arneodo's X(t) component which is 1.3790017739e-10 and maximum residuals is 6.6562602866e+00 with MAE 1.9302504058e+00. Similarly, in Figure (19c), the minimum absolute error deviation of Adams vs E-RK is 4.1141859919e-09 and maximum residuals is 6.9159928211e+00 with MAE 2.0113364328e+00 for Arneodo's X(t) component. In Figure (19d), we observe a minimum residual of Adams vs I-RK of 5.9559297494e-09 and maximum residual of .6919431044e+00 with MAE 1.9636032449e+00 in Arneodo's X(t) component. Figure 20a exhibits absolute error between reference Adams Numerical Computing (ANC) Procedure across various numerical techniques including BDF, E-RK and I-RK for the Arneodo's Y(t). Figure 20(b) exhibits absolute error of Arneodo's Y(t) compartment with the minimum residuals of Adams vs BDF is 8.4851278781e-10 and maximum residuals is 1.0702299044e+01 with MAE 2.1049407668e+00. Similarly, Figure 20(c) the minimum residuals of Adams vs E-RK is 4.9398699575e-09 and maximum residuals is 1.1111816437e+01 with MAE 2.0244326670e+00, Figure 20(d) the minimum residuals of Adams vs I-RK is 6.5951956119e-09 and maximum residuals is 1.0748194708e+01 with MAE 2.0444278415e+00. Similarly, Figure 21a exhibits absolute error between reference Adams Numerical Computing (ANC) Procedure across various numerical techniques including BDF, E-RK and I-RK for the Arneodo's Z(t). Figure 21(b) exhibits absolute error of Arneodo's Z(t) compartment with the Minimum residuals error of Adams vs BDF is 2.4438515100e-10 and maximum residuals is 1.8571419828e+01 with MAE 3.9385665605e+00. Similarly, the minimum residuals of Adams vs E-RK which is 2.0729014283e-08 and maximum residuals is 2.1034817721e+01 with MAE 3.7247976958e+00, The minimum residuals of Adams vs I-RK which is 7.7073988025e-09 and maximum residuals are 1.8929289471e+01 with MAE 3.8281942959e+00.



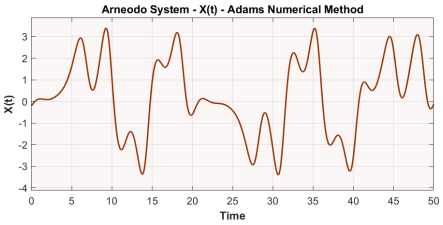
(7a) Trajectory evolution of function X(t) of Arneodo's system using Adams method



(7b) $0 \leq t \leq 150$

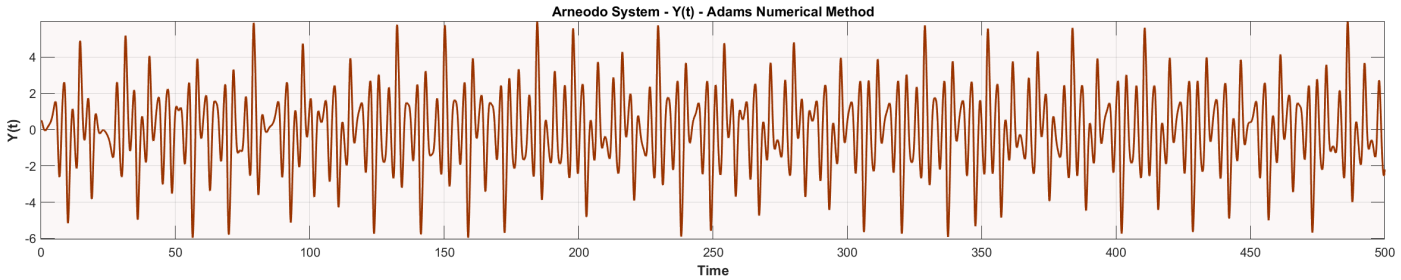


(7c) $0 \leq t \leq 100$

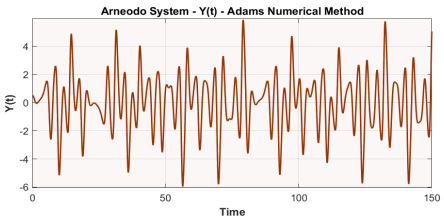


(7d) $0 \leq t \leq 50$

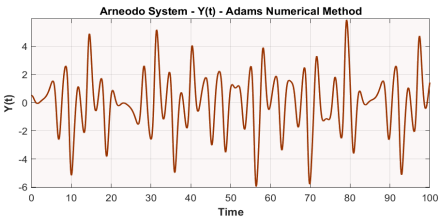
Fig. 7 Time response of the Arneodo's chaotic system state X(t) over $0 \leq t \leq 500$ obtained by Adams method.



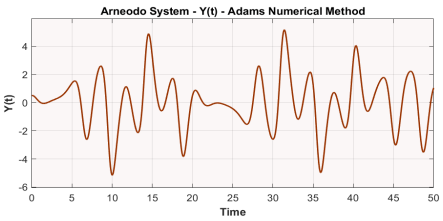
(8a) Trajectory evolution of function Y(t) of Arneodo's system using Adams method



(8b) $0 \leq t \leq 150$

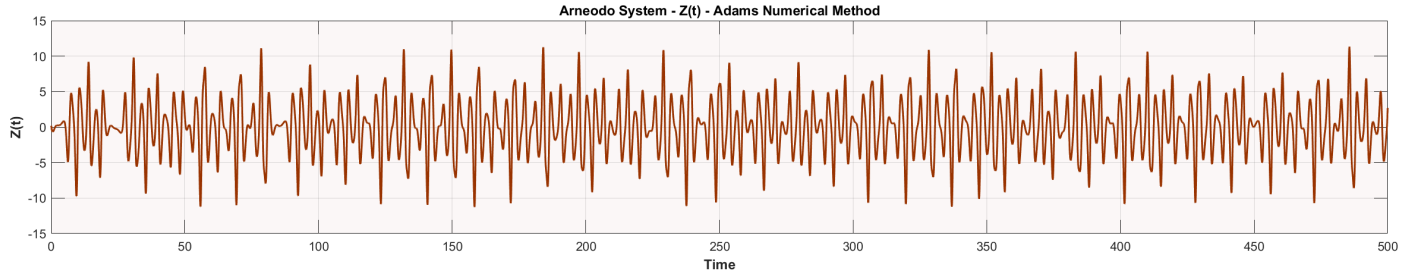


(8c) $0 \leq t \leq 100$

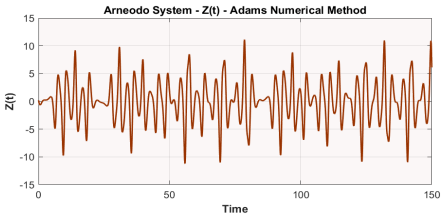


(8d) $0 \leq t \leq 50$

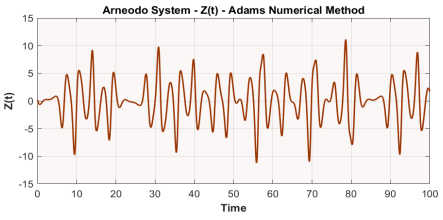
Fig. 8 Time response of the Arneodo's chaotic system state Y(t) over $0 \leq t \leq 500$ obtained by Adams method.



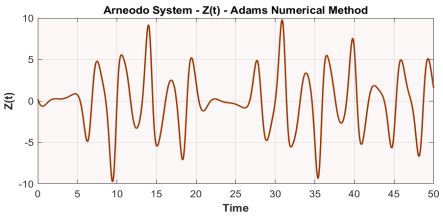
(9a). Trajectory evolution of function Z(t) of Arneodo's system using Adams method



(9b) $0 \leq t \leq 150$

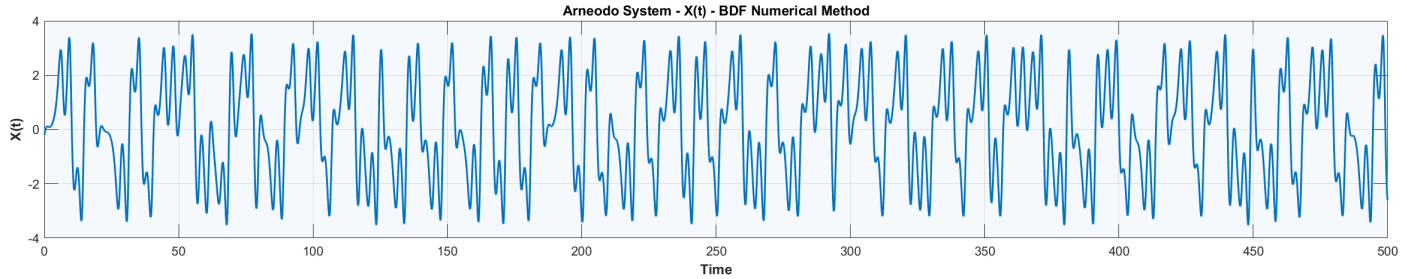


(9c) $0 \leq t \leq 100$

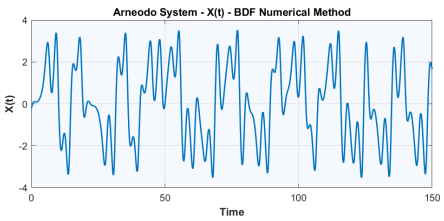


(9d) $0 \leq t \leq 50$

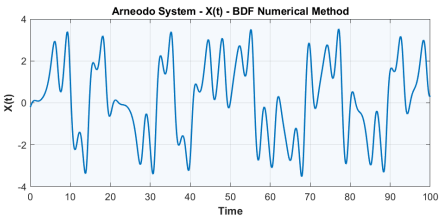
Fig. 9 Time response of the Arneodo chaotic system state Z(t) over $0 \leq t \leq 500$ obtained by Adams method.



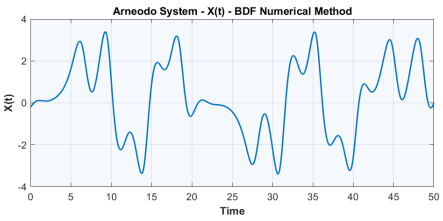
(10a) Trajectory evolution of function X(t) of Arneodo's system using BDF method



(10b) $0 \leq t \leq 150$

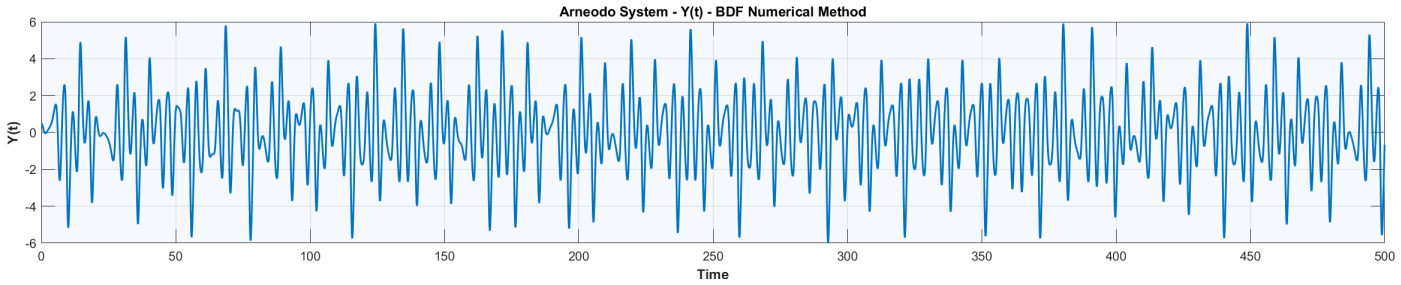


(10c) $0 \leq t \leq 100$

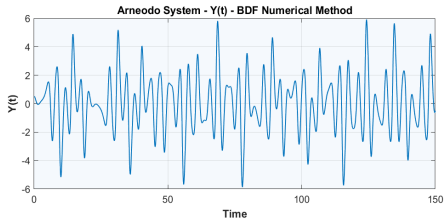


(10d) $0 \leq t \leq 50$

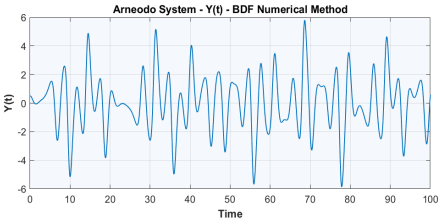
Fig. 10 Time response of the Arneodo's chaotic system state X(t) over $0 \leq t \leq 500$ obtained by BDF method.



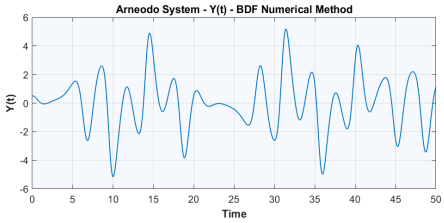
(11a) Trajectory evolution of function Y(t) of Arneodo's system using BDF method



(11b) $0 \leq t \leq 150$

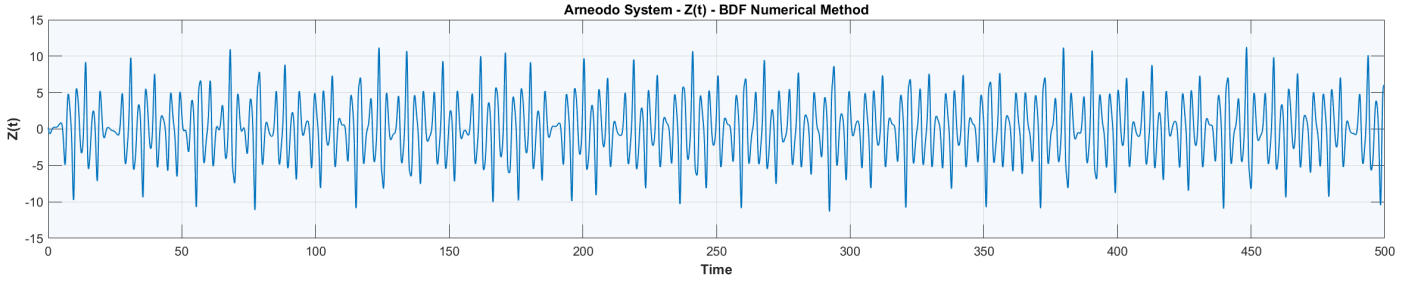


(11c) $0 \leq t \leq 100$

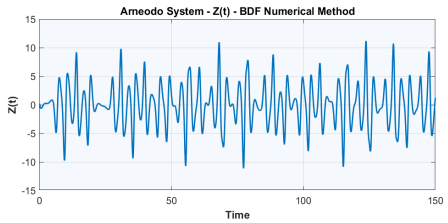


(11d) $0 \leq t \leq 50$

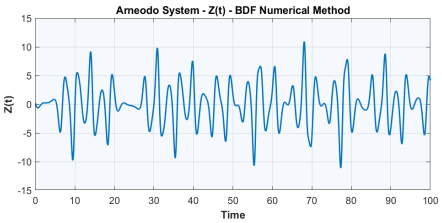
Fig. 11 Time response of the Arneodo's chaotic system state Y(t) over $0 \leq t \leq 500$ obtained by BDF method.



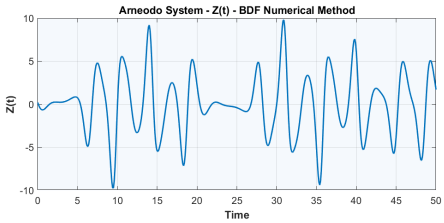
(12a) Trajectory evolution of function Z(t) of Arneodo's system using BDF method



(12b) $0 \leq t \leq 150$

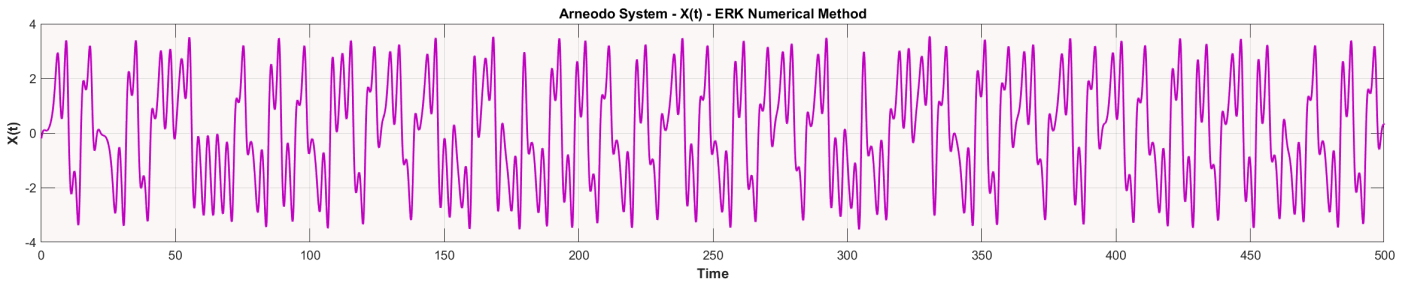


(12c) $0 \leq t \leq 100$

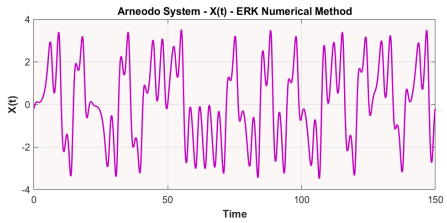


(12d) $0 \leq t \leq 50$

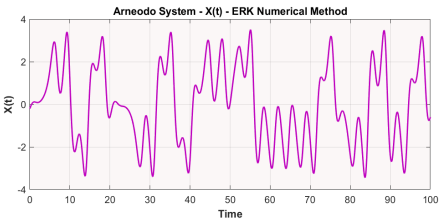
Fig. 12 Time response of the Arneodo's chaotic system state Z(t) over $0 \leq t \leq 500$ obtained by BDF method.



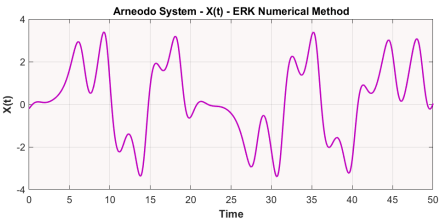
(13a) Trajectory evolution of function X(t) of Arneodo's system using E-RK method



(13b) $0 \leq t \leq 150$

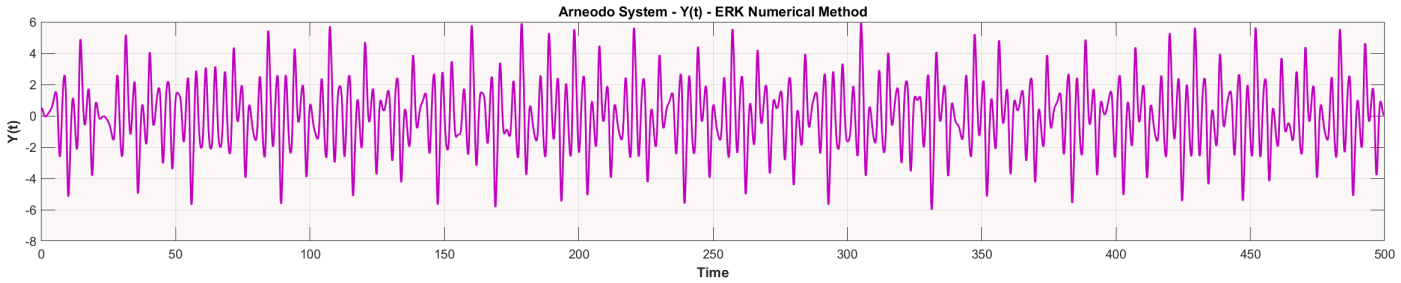


(13c) $0 \leq t \leq 100$

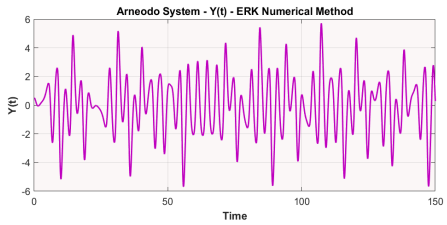


(13d) $0 \leq t \leq 50$

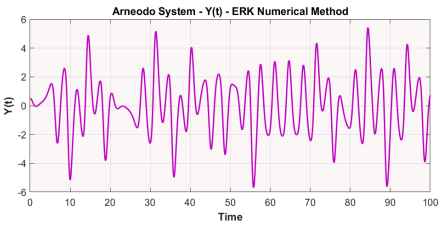
Fig. 13 Time response of the Arneodo's chaotic system state X(t) over $0 \leq t \leq 500$ obtained by E-RK method.



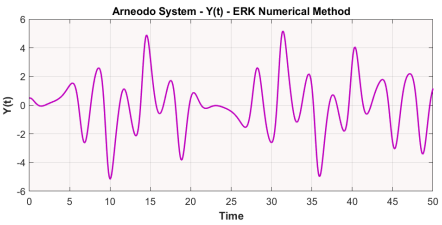
(14a) Trajectory evolution of function Y(t) of Arneodo's system using E-RK method



(14b) $0 \leq t \leq 150$

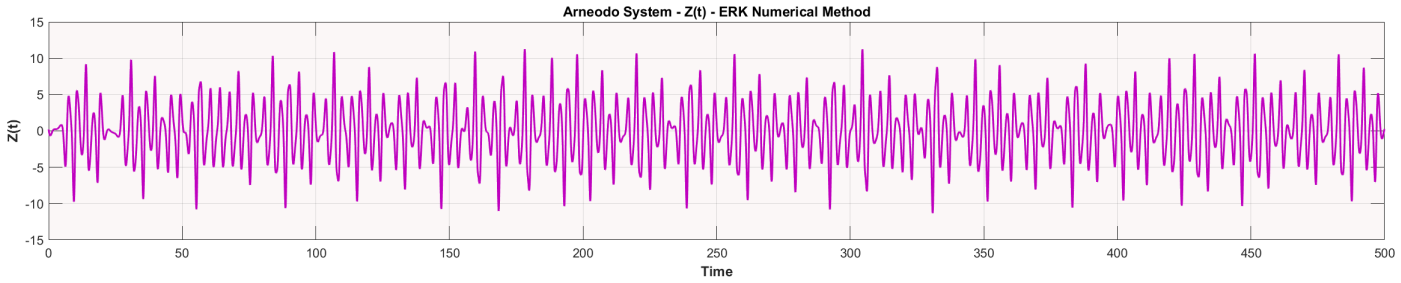


(14c) $0 \leq t \leq 100$

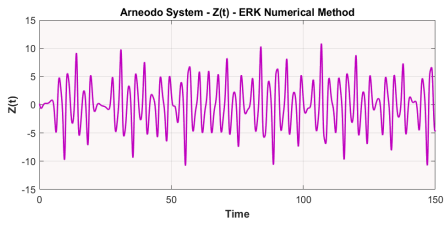


(14d) $0 \leq t \leq 50$

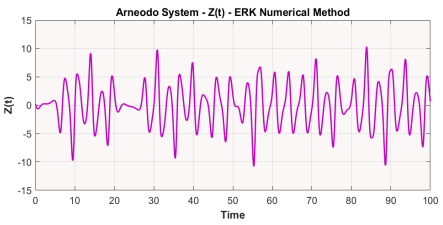
Fig. 14 Time response of the Arneodo's chaotic system state Y(t) over $0 \leq t \leq 500$ obtained by E-RK method.



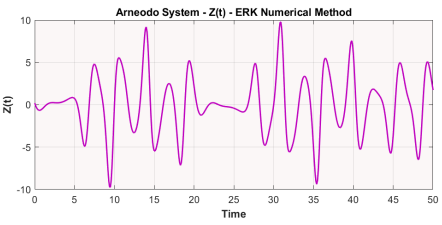
(15a) Trajectory evolution of function Z(t) of Arneodo's system using E-RK method



(10b) $0 \leq t \leq 150$

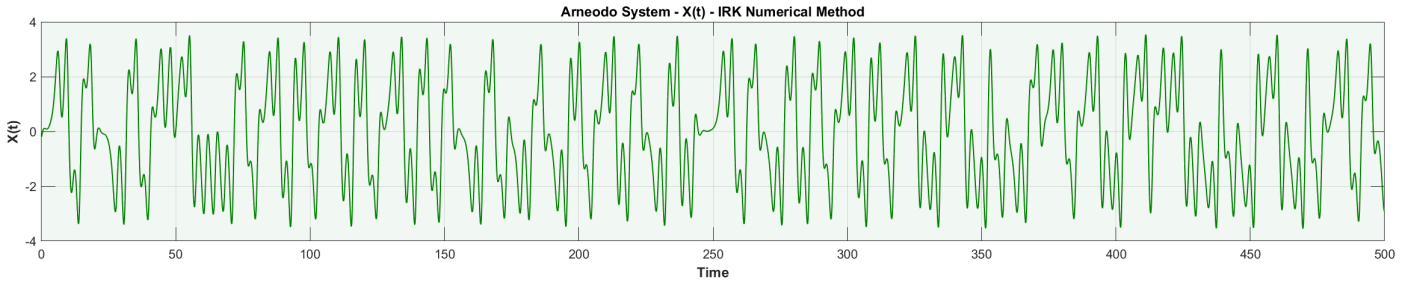


(10c) $0 \leq t \leq 100$

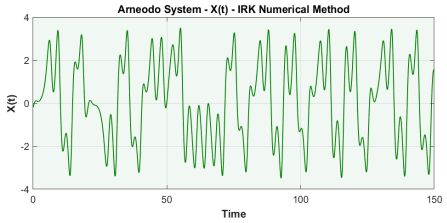


(10d) $0 \leq t \leq 50$

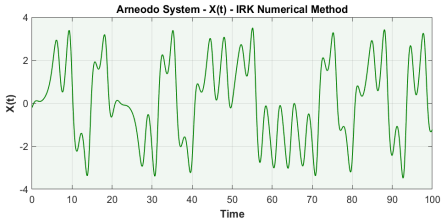
Fig. 15 Time response of the Arneodo's chaotic system state Z(t) over $0 \leq t \leq 500$ obtained by E-RK method.



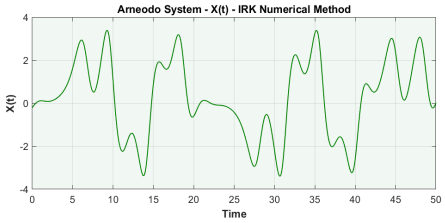
(16a) Trajectory evolution of function X(t) of Arneodo's system using I-RK method



(16b) $0 \leq t \leq 150$

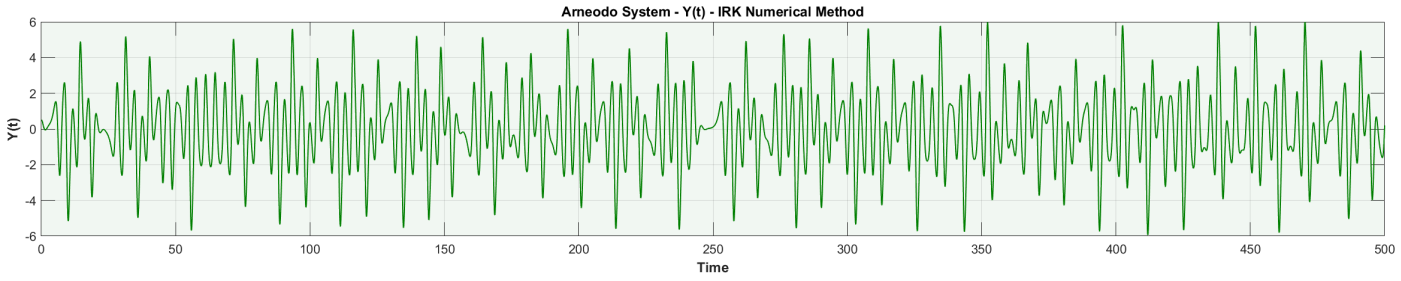


(16c) $0 \leq t \leq 100$

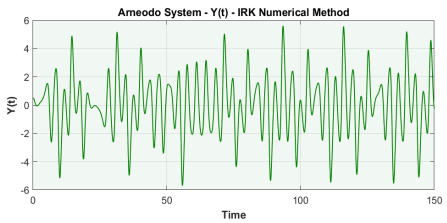


(16d) $0 \leq t \leq 50$

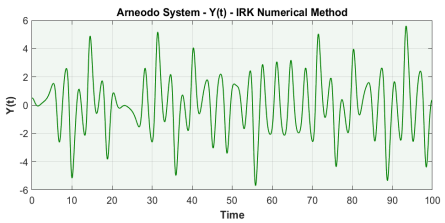
Fig. 16 Time response of the Arneodo's chaotic system state X(t) over $0 \leq t \leq 500$ obtained by I-RK method.



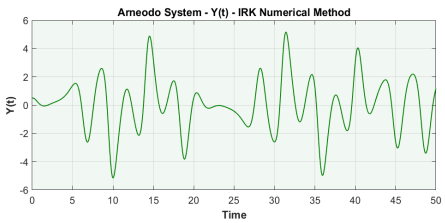
(17a) Trajectory evolution of function Y(t) of Arneodo's system using I-RK method



(17b) $0 \leq t \leq 150$

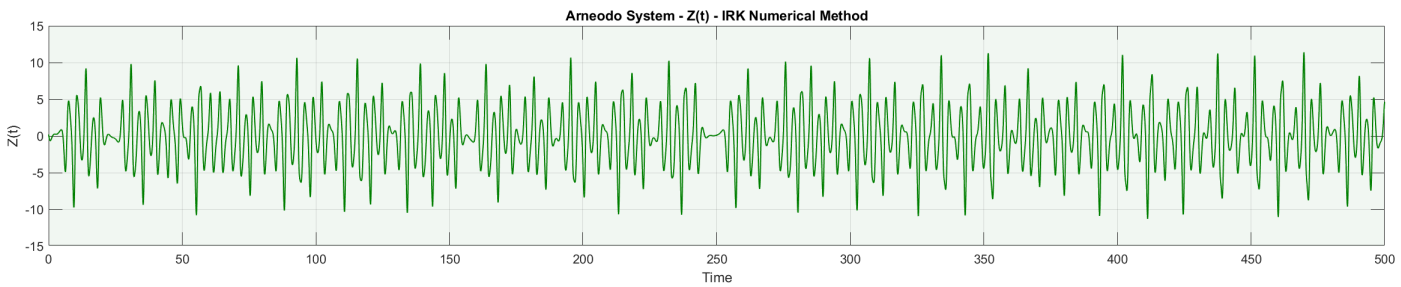


(17c) $0 \leq t \leq 100$

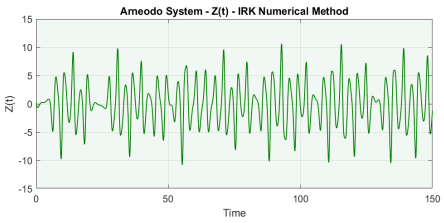


(17d) $0 \leq t \leq 50$

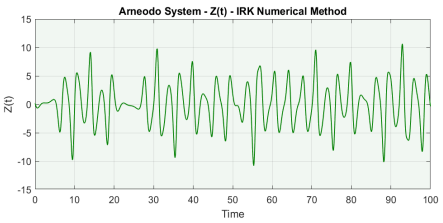
Fig. 17 Time response of the Arneodo's chaotic system state Y(t) over $0 \leq t \leq 500$ obtained by I-RK method.



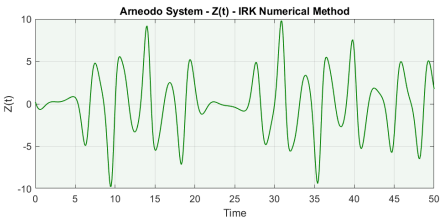
(18a) Trajectory evolution of function Z(t) of Arneodo's system using I-RK method



(18b) $0 \leq t \leq 150$

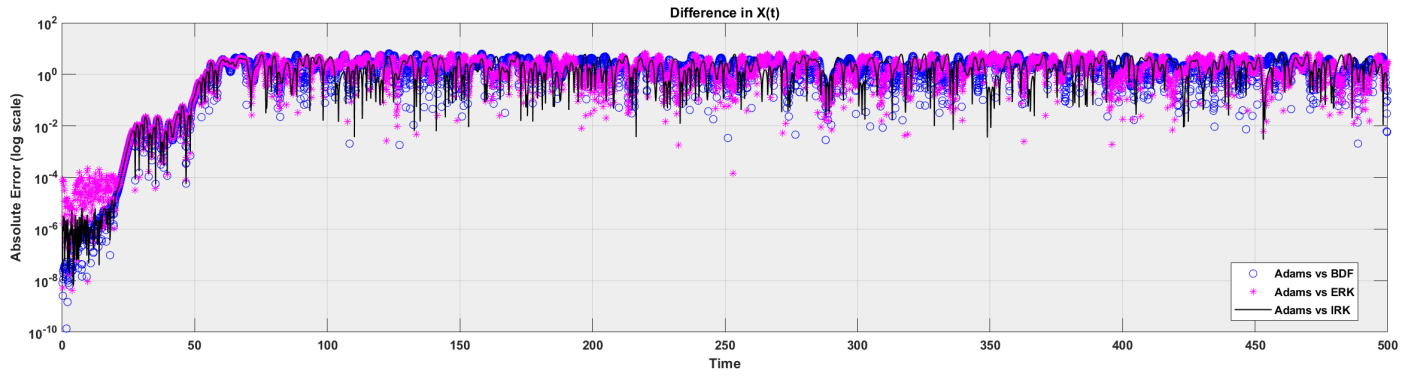


(18c) $0 \leq t \leq 100$

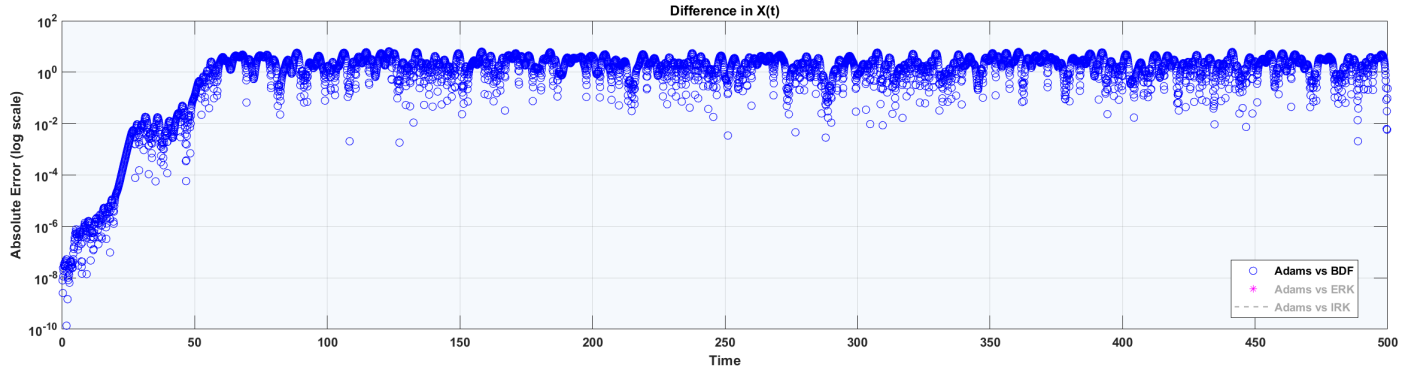


(18d) $0 \leq t \leq s50$

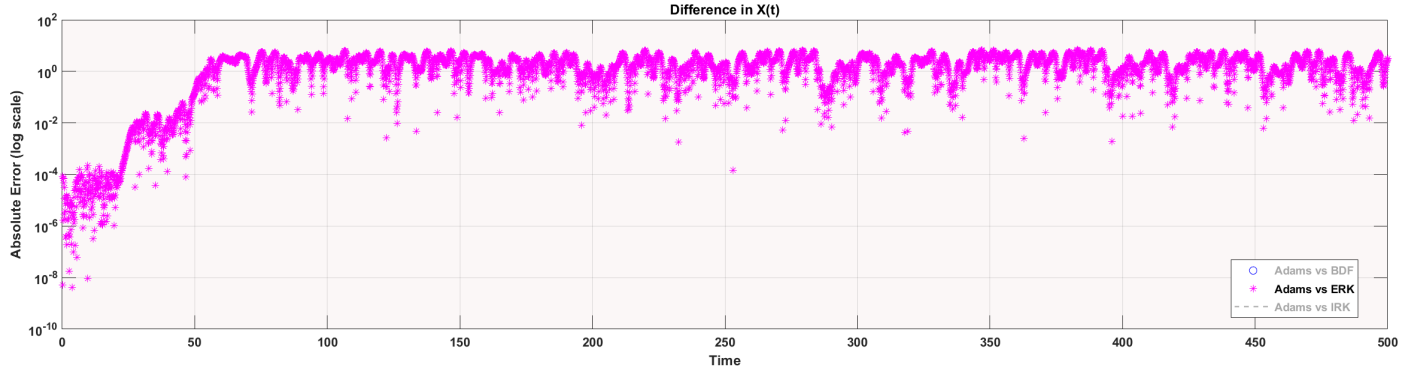
Fig. 18 Time response of the Arneodo's chaotic system state Z(t) over $0 \leq t \leq 500$ obtained by I-RK method.



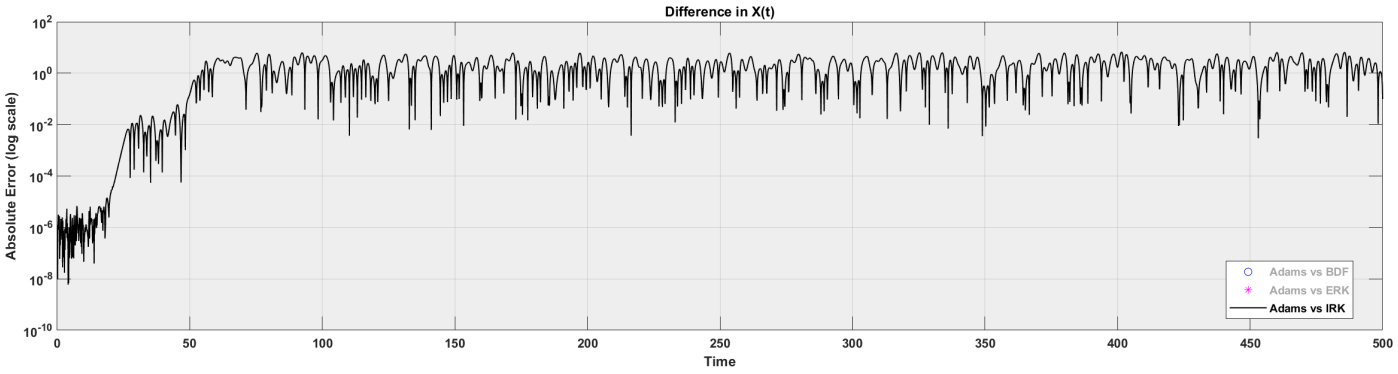
(19a) Comparison graph for absolute error between Adams vs BDF, Adams vs E-RK and Adams vs I-RK for X(t)



(19b) Adams vs BDF

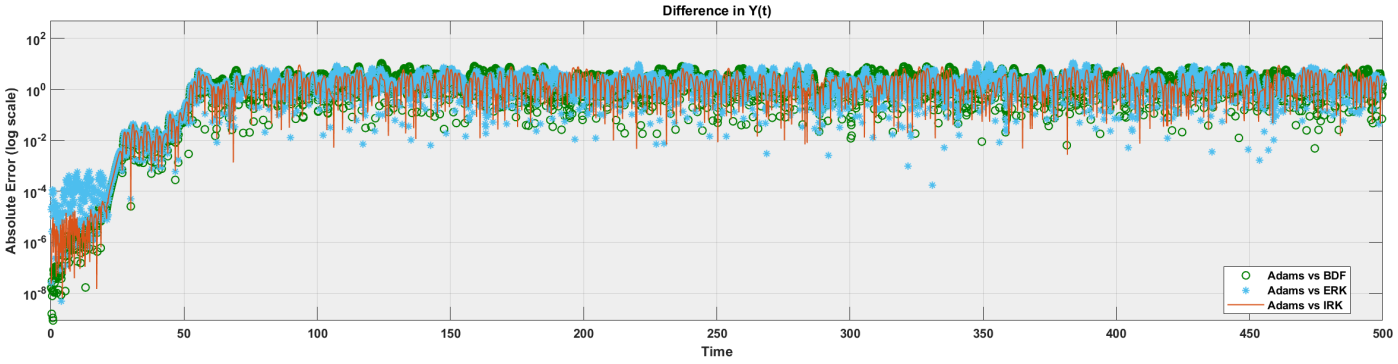


(19c) Adams vs E-RK

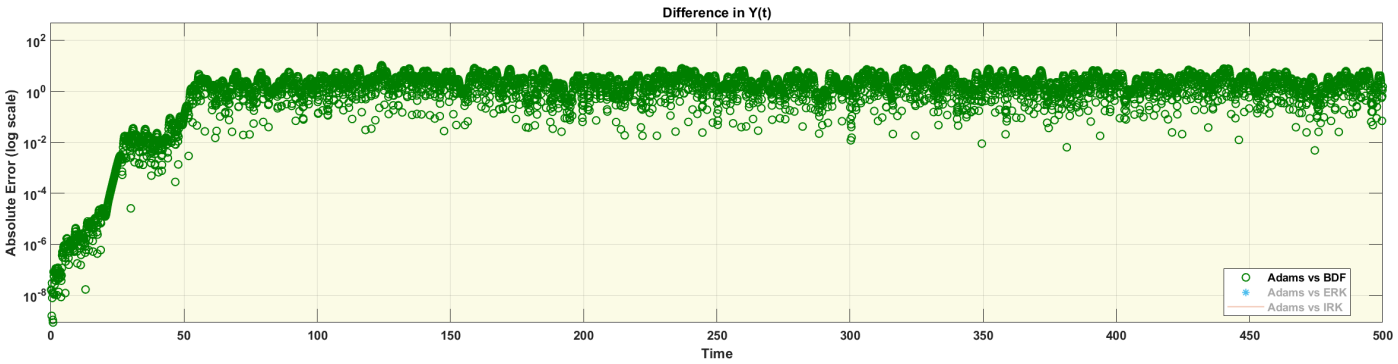


(19d) Adams vs I-RK

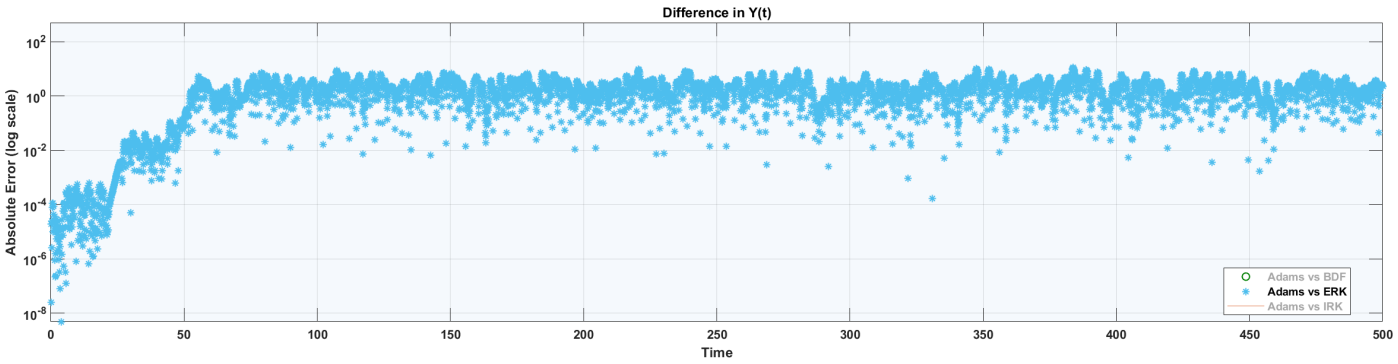
Fig. 19 Absolute error between Adams vs other numerical solution with BDF, E-RK, and I-RK for X(t)



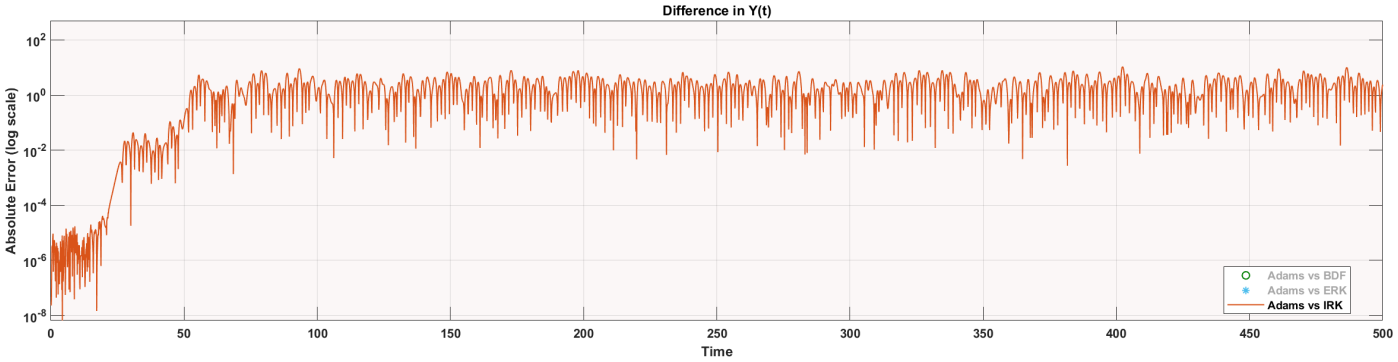
(20a) Comparison graph for absolute error between Adams vs BDF Adams vs E-RK and Adams vs I-RK for Y(t)



(20b) Adams vs BDF



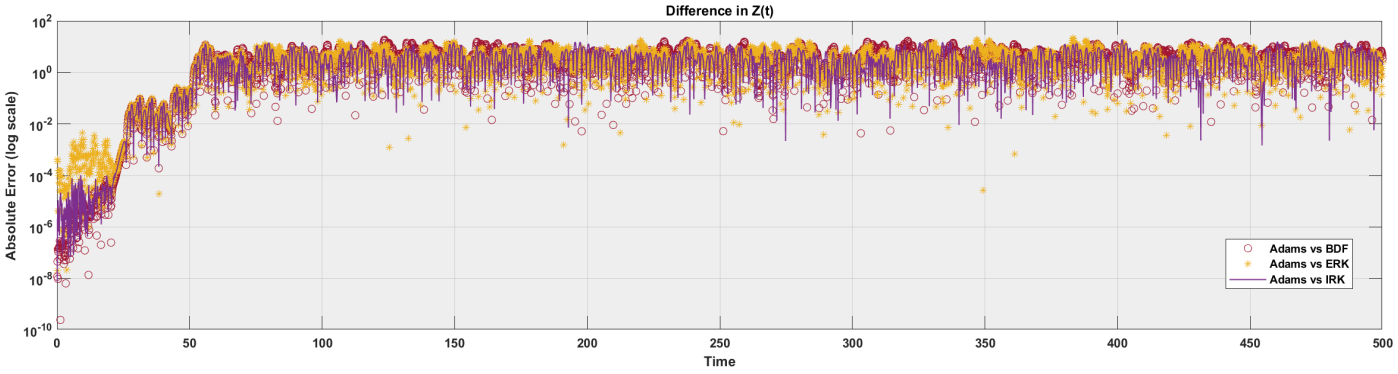
(20c) Adams vs E-RK



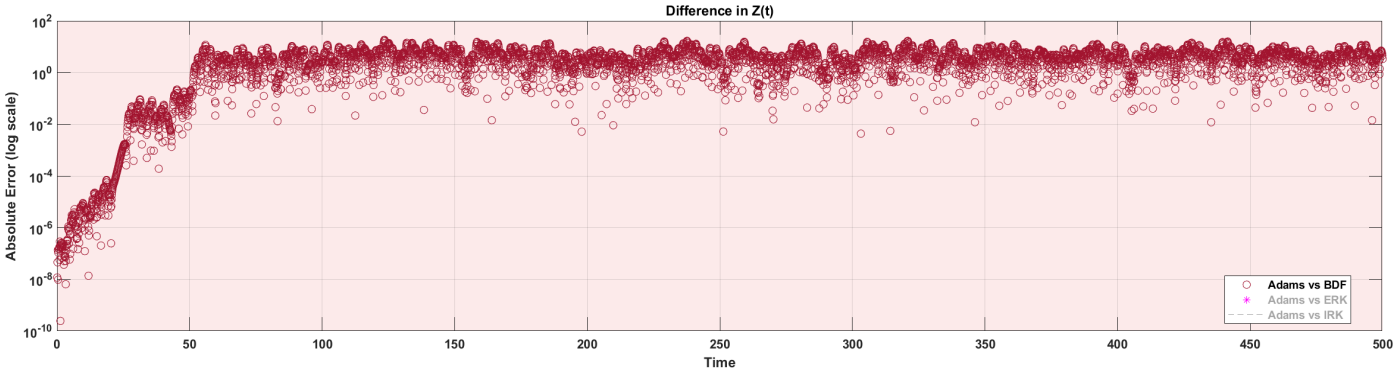
(20d) Adams vs I-RK

Fig. 20 Absolute error between Adams vs other numerical solution with BDF, E-RK, and I-RK for Y(t)

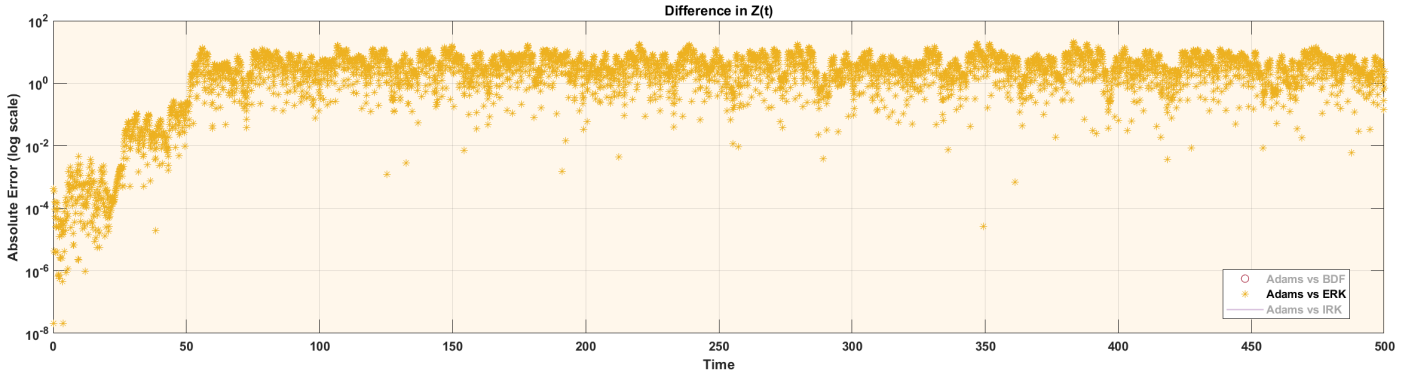
Comparison graphs representing the absolute error of Adams vs BDF Adams vs E-RK and Adams vs I-RK methods for three different functions: (a) *X(t)*, (b) *Y(t)*, and (c) *Z(t)*. Each graph illustrates the variation of absolute error with respect to tfor the compared methods



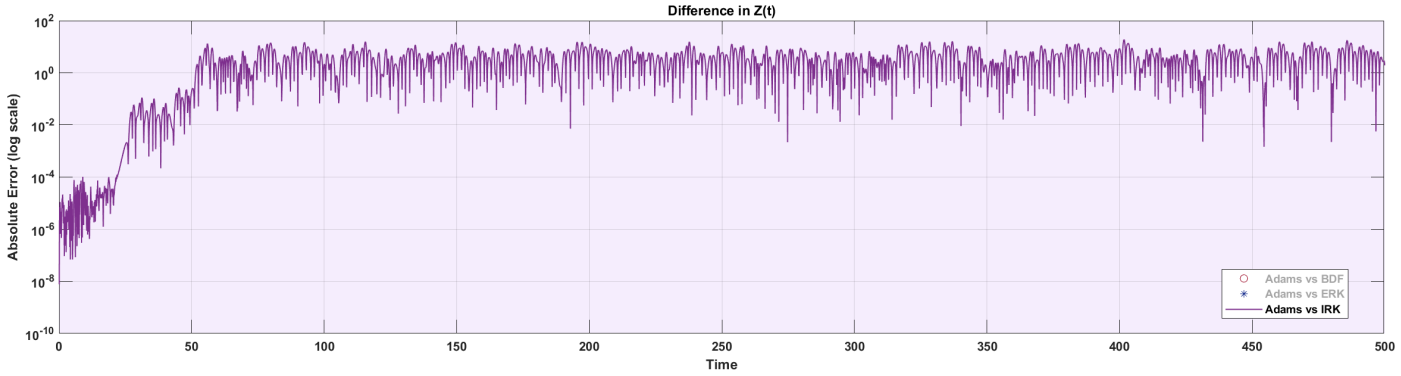
(21a) Comparison graph for absolute error between Adams vs BDF Adams vs E-RK and Adams vs I-RK for Z(t)



(21b) Adams vs BDF



(21c) Adams vs E-RK



(21d) Adams vs I-RK

Fig. 21 Absolute error between Adams vs other numerical solution with BDF, E-RK, and I-RK for Y(t)

5. CONCLUSION

This study demonstrates an effective numerical analysis of Arneodo's system that exhibits complex chaotic behavior with all methods implemented namely the Adams, BDF, E-RK and I-RK methods. The comparative studies of the Adams vs BDF, Adams vs E-RK, and Adams vs I-RK procedure are portrayed with absolute residual analysis of the three compartmental Arneodo's system X(t), Y(t), Z(t). The results show that the Adams, BDF, E-RK, and I-RK numerical schemes produce comparable chaotic responses, although solver-dependent deviations are observed. The very small minimum residual values, ranging from 10^{-9} to 10^{-8}, indicate that the numerical methods agree very closely at certain time instants. The maximum residuals, which reach approximately 5.5 to 5.8, show that noticeable deviations occur during the simulation. These deviations are expected in chaotic systems because small differences introduced by numerical schemes can grow with time due to the sensitive dependence on initial conditions and nonlinear system dynamics. Among the comparisons, the Adams–E-RK pair gives the lowest mean absolute error, suggesting better average agreement for the X(t) response. On the other hand, the Adams–BDF comparison gives the lowest mean square error, indicating slightly better control over squared-error accumulation. The residual results confirm that all numerical methods successfully capture the bounded chaotic behavior of X(t). The differences between the solvers do not necessarily indicate failure of the methods; rather, they reflect the natural sensitivity of chaotic systems to numerical approximation. Since an exact analytical solution is not available, these values should be interpreted as numerical residuals between computational schemes rather than exact physical errors. Therefore, the error analysis supports the reliability of the obtained chaotic response while also highlighting the importance of using multiple numerical methods for validation.

5.1 Limitations & Future Work

In this study, we merely simulated Arneodo's system numerically using four prestigious numerical schemes. In future, we may extend these to hybrid computationally intelligent schemes [41-42] in order to solve the Arneodo's system. Moreover, in this study, the point of interest is in the classical ODE form of the 3D Arneodo's system. Feature additions such as the effect of delay, the fractional-order memory, stochastic noise elements can be induced across the classical Arneodo's system to enhance the properties of the dynamical system. More aggressive numerical simulations may be run to study the nature of the system and its chaotic attractor properties. Arneodo's chaotic system applications in security/encryption should be explored as well. Controlling chaos posed by Arneodo's attractor using traditional as well as Reinforcement Learning based intelligent methodologies should be considered in the future as well. Moreover, the chaotic nature of Arneodo's system should be juxtaposed across other famous chaotic attractors such as Lorenz, Rossler and Chua based attractors.

REFERENCES

[1] Owolabi, K.M. and Atangana, A., 2018. "Chaotic behaviour in system of noninteger-order ordinary differential equations." *Chaos, Solitons & Fractals,* **115**, pp.362-370.

[2] Shinbrot, T., Ditto, W., Grebogi, C., Ott, E., Spano, M. and Yorke, J.A., 1992. "Using the sensitive dependence of chaos (the "butterfly effect") to direct trajectories in an experimental chaotic system." *Physical review letters,* **68**(19), p.2863.

[3] Eckmann, J.P. and Ruelle, D., 1985. "Ergodic theory of chaos and strange attractors." *Reviews of modern physics,* **57**(3), p.617.

[4] Poincaré, H., 1890. "Sur le problème des trois corps et les équations de la dynamique." *Acta mathematica,* **13**(1), pp.A3-A270.

[5] Poincaré, H., 1893. "Les méthodes nouvelles de la mécanique céleste (Vol. 2). " *Gauthier-Villars.*

[6] Arneodo, A., Coullet, P. and Tresser, C., 1981. "Possible new strange attractors with spiral structure, qaCommunications in Mathematical Physics," **79**(4), 573–579.

[7] Toth, Z., Buizza, R. and Feng, J., 2026. "Weather forecasting: What sets the forecast skill horizon?." *In Sub-Seasonal to Seasonal Prediction* (pp. 21-68). Elsevier.

[8] Chakraborty, D., Mohan, A.T. and Maulik, R., 2026. "Binned spectral power loss for improved prediction of chaotic systems." *Journal of Computational Physics,* p.114866.

[9] Xian, Y., Wang, X., Teng, L., Yan, X., Li, Q. and Wang, X., 2022. "Cryptographic system based on double parameters fractal sorting vector and new spatiotemporal chaotic system." *Information Sciences,* **596**, pp.304-320.

[10] Jiang, C., Ye, Y., Zhang, F., Kou, L., Bao, H., Zhang, J. and Liu, H., 2025. "Hardware implementation and information security application of a novel chaotic system with a cubic memristor and complex parameters." *Chaos, Solitons & Fractals,* **196**, p.116379.

[11] Volos, C.K., Kyprianidis, I.M. and Stouboulos, I.N., 2013. "Experimental investigation on coverage performance of a chaotic autonomous mobile robot." *Robotics and Autonomous Systems,* **61**(12), pp.1314-1322.

[12] Buscarino, A., Camerano, C., Fortuna, L. and Frasca, M., 2010. "Chaotic mimic robots." *Philosophical Transactions of the Royal Society A: Mathematical, Physical and Engineering Sciences,* **368**(1918), pp.2179-2187.

[13] Akgul, A., Hussain, S. and Pehlivan, I., 2016. "A new three-dimensional chaotic system, its dynamical analysis and electronic circuit applications." *Optik,* **127**(18), pp.7062-7071.

[14] Babajans, R., Cirjulina, D. and Kolosovs, D., 2025. "Field-programmable gate array-based chaos oscillator implementation for analog–discrete and discrete–analog chaotic synchronization applications." *Entropy,* **27**(4), p.334.

[15] Syed, F.A., Fang, K.T., Kiani, A.K., Shoaib, M. and Raja, M.A.Z., 2025. "Design of Neuro-Stochastic bayesian networks for nonlinear chaotic differential systems in financial mathematics." *Computational Economics,* **65**(1), pp.241-270.

[16] Reyes-Ortiz, N., Clemente-Lopez, D., de Jesus Rangel-Magdaleno, J., Rosales-Nunez, S. and Barron-Zambrano, J.H., 2026. "Physical design of a 32-bit RISC-V based microprocessor: A proof of concept for chaotic systems implementation." *Computers and Electrical Engineering,* **134**, p.111152.

[17] Liu, X., Li, C., Ge, S.S. and Li, D., 2022. "Time-synchronized control of chaotic systems in secure communication." *IEEE Transactions on Circuits and Systems I: Regular Papers,* **69**(9), pp.3748-3761.

[18] Ranstrom, T., Jebreil, O., Razak, F.A., Yilmaz, Y. and Mumcu, G., 2026. "Analytical and Experimental Validation of Wireless Authentication through Enhanced RF Fingerprints of Chaotic Antenna Arrays." *IEEE Transactions on Information Forensics and Security.*

[19] Su, H., Wang, J., Ma, J., Zhang, Y., Zhang, J. and Wang, M., 2026. "A photonic-assisted joint radar and communication system based on LFM-DCSK waveform." *Optics Letters,* **51**(5), pp.1152-1155.

[20] Szczęsna, A., Augustyn, D.R., Josiński, H., Harężlak, K., Świtoński, A. and Kasprowski, P., 2023. "Chaotic biomedical time signal analysis via wavelet scattering transform." *Journal of Computational Science,* **72**, p.102080.

[21] El-Diraby, T.E., 2013. "Civil infrastructure decision making as a chaotic sociotechnical system: Role of information systems in engaging stakeholders and democratizing innovation." *Journal of infrastructure systems,* **19**(4), pp.355-362.

[22] Park, S.J. and Choi, D.H., 2026. "Bifurcation and Chaos Analysis in Nonlinear Mechanical Systems using Lyapunov Exponents and Phase Space Reconstruction." *Computer Science Bulletin,* **9**(1), pp.28-35.

[23] Papadopoulou, M.S., 2026. "Chaotic Mobile Robot for Coverage Path Planning Scenarios Using Lorenz System." *In International Interdisciplinary Chaos Symposium on Chaos and Complex Systems* (pp. 119-129). Springer, Cham.

[24] Liu, Z., Zhang, Y., Yang, S. and Lyu, Y., 2023. "Multivariate cooperative internal mode control of RBF neural network for power system chaos suppression." *IEEE Access,* **11**, pp.139112-139120.

[25] Mehmood, K., Khan, Z.A., Chaudhary, N.I., Cheema, K.M., Siddiqui, B. and Raja, M.A.Z., 2024. "Design of chaotic Young's double slit experiment optimization heuristics for identification of nonlinear muscle model with key term separation." *Chaos, Solitons & Fractals,* **189**, p.115636.

[26] Xu, X., Zhang, L., Trovati, M., Palmieri, F., Asimakopoulou, E., Johnny, O. and Bessis, N., 2021. "PERMS: An efficient rescue route planning system in disasters." *Applied Soft Computing,* **111**, p.107667.

[27] Vitvitskyi, A., Boratko, M., Grcic, M., Pascanu, R., Shah, D. and Veličković, P., 2026. "Mining Generalizable Activation Functions." *arXiv preprint* arXiv:2602.05688.

[28] Höffmann, M., Clemens, J., Stronzek-Pfeifer, D., Simonelli, R., Serov, A., Schettino, S., Runge, M., Schill, K. and Büskens, C., 2022, "December. Coverage path planning and precise localization for autonomous lawn mowers." *In 2022 Sixth IEEE International Conference on Robotic Computing* (IRC) (pp. 238-242). IEEE.

[29] Mehmood, K., Chaudhary, N.I., Khan, Z.A., Cheema, K.M., Raja, M.A.Z., Alshamrani, S.S. and Alshmrany, K.M., 2025. "Design of Chaos Induced Aquila Optimizer for Parameter Esti-

mation of Electro-Hydraulic Control System." *Computer Modeling in Engineering & Sciences* (CMES), **143**(2).

[30] Aghababa, M.P., 2012. "Chaos in a fractional-order micro-electro-mechanical resonator and its suppression. *Chinese Physics B,* **21**(10), p.100505.

[31] Sambas, A., Vaidyanathan, S., Tlelo-Cuautle, E., Zhang, S., Guillen-Fernandez, O., Sukono, Hidayat, Y. and Gundara, G., 2019. "A novel chaotic system with two circles of equilibrium points: Multistability, electronic circuit and FPGA realization." *Electronics,* **8**(11), p.1211.

[32] Mao, Y. and Chen, G., 2005. "Chaos-based image encryption. In Handbook of geometric computing: applications in pattern recognition, computer vision, neuralcomputing, and robotics (pp. 231-265)." *Berlin,* Heidelberg: Springer Berlin Heidelberg.

[33] Gokyildirim, A., Akgul, A., Calgan, H. and Demirtas, M., 2024. "Parametric fractional-order analysis of Arneodo chaotic system and microcontroller-based secure communication implementation." *AEU-International Journal of Electronics and Communications,* **175**, p.155080.

[34] Zhao, H., Yan, S., Yu, Q., Liu, C. and Lu, Z., 2025, "February. Projective Synchronization Control of the Arneodo System and Coullet System." *In International Conference on Mechanical Design and Simulation* (pp. 843-851). Singapore: Springer Nature Singapore.

[35] Emin, B., Akgul, A., Horasan, F., Gokyildirim, A., Calgan, H. and Volos, C., 2024. "Secure encryption of biomedical images based on Arneodo chaotic system with the lowest fractional-order value." *Electronics,* **13**(11), p.2122.

[36] Akgül, A., Yaz, M. and Emin, B., 2025. "Chaos-based approaches to data security: Analysis of incommensurate fractional-order Arneodo chaotic system and engineering application on a microcomputer." *Integration,* **102**, p.102355.

[37] Khalid, T.A., Taha, N.E., Juma, M.Y., Elmahi, M., Hagabdulla, N.H. and Ali, I.A., 2026. "Order Modulation for Chaos Control and Hybrid Synchronization in a Variable-Order Fractional Arneodo System: Spectral Stability and Numerical Validation." *Fractal and Fractional.*

[38] Liu, S., Wang, Q., Liu, C., Sun, Y. and He, L., 2023. "Natural Exponential and Three-Dimensional Chaotic System." *Advanced Science,* **10**(15), p.2204269.

[39] Elbadri, M., Al-kuleab, N., Saadeh, R., H. Abdalla, A., Jazmati, M.S., A. Abdoon, M. and Hafez, M., 2026. "Study of the Variable-Order Fractional Arneodo System: Bifurcation, Chaos, and Dynamic Behavior." *Fractal and Fractional,* **10**(5), p.296.

[40] Butcher, J.C., 2016. "Numerical methods for ordinary differential equations." *John Wiley & Sons.*

[41] Syed, F.A., Fang, K.T., Kiani, A.K., Shoaib, M. and Raja, M.A.Z., 2025. "Design of Exogenous Neuro-Structure for Dynamical Analysis of Nonlinear Fractional Financial Crime Systems." *International Journal of Information Technology & Decision Making,* **24**(06), pp.1849-1903.

[42] Syed, F.A., Fang, K.T., Kiani, A.K., Shih, D.H., Shoaib, M. and Zahoor Raja, M.A., 2025. "Novel intelligent supervised neuro-structures for nonlinear financial crime differential systems." *Modern Physics Letters B,* **39**(01), p.2450399.